

# Schlussbericht

**Zuwendungsempfänger: Universität Heidelberg**

**Forderkennzeichen: 03SHE2HD**

**Vorhabenbezeichnung: Molekulare Dynamik von biologisch relevanten Steroiden in Membranen**

**Laufzeit des Vorhabens: 01.04.2001 - 31.03.2004**

**Berichtszeitraum: 01.04.2001 - 31.03.2004**

## 1 Einleitung

Lipid membranes of eukaryotic cells have a complex composition consisting of hundreds of different lipids and proteins, plus cholesterol or closely related sterols. In mammalian cells cholesterol has been found to account for up to 50% of the lipid concentration in the membrane. Cholesterol covers a wide range of roles in human cells; it serves as being the precursor for the synthesis of hormones and numerous other biologically important molecules [1, 2, 3], but it is also influencing the physicochemical properties of biomembranes. The effect of cholesterol and other biologically important sterols such as lanosterol and ergosterol to functional, structural and dynamical membrane properties has received sizeable attention in the past decades. Cholesterol has been shown to optimize the physical properties of the membrane and regulate its fluidity [4], but also other possible roles, such as its role in signal transduction [5] and ion permeability [6] are under investigation. Ergosterol (provitamin D<sub>2</sub>) can be found in the membranes of fungi, yeasts and protozoans and lanosterol, the evolutionary precursor of cholesterol, is the major constituent of prokaryotic cell membranes.

Although ergosterol and lanosterol are structurally very similar to cholesterol, only cholesterol has been chosen by evolution to be the major constituent of the eukaryotic plasma membranes. The process of conversion of lanosterol to cholesterol in mammalian cells requires 19 enzymatic steps. Therefore, an intriguing question concerns elucidating the particular characteristics of cholesterol, which have led to its evolutionary selection in eukaryotic plasma membranes, even in presence of structurally very similar precursors. It has been postulated that evolution has selected cholesterol because it optimizes the physical properties of the membrane [7]. Cholesterol, compared to its analogues, has been shown to reduce the permeability and to increase molecular ordering as well as lateral diffusion of phospholipids [8, 9] Moreover, it dramatically influences the gel-liquid crystal phase transition of phospholipids by introducing a new thermodynamically stable region of coexistence between the liquid and gel phase, the liquid-disordered (ld) phase.

[10, 11, 12]. Although substantial work has focused on this area of research, it is still unclear which specific parts of this molecule provide this optimization.

The physical properties of eucaryotic plasma membranes can be reproduced and studied with model biological membranes [1, 13, 14]. Experimental as well as computational studies of these systems have been used to shed light on the nature of membrane-sterol interactions. Experimental studies aimed at monitoring the way by which cholesterol affects the membrane properties very often lack sufficient resolution for investigating the underlying molecular interactions that drive the observed properties. Using Molecular Dynamics (MD) simulations, it is possible to interpret experimental results of complex membrane systems and gain insight on their interactions at the microscopic level. The field of lipid bilayer simulations is growing rapidly and more recently the level of complexity is increasing with explicit inclusion of membrane proteins [15, 16, 17, 18] and cholesterol [19, 20, 21, 22] in the simulated systems.

## 2 Wissenschaftlicher und technischer Stand. Voraussetzungen

Our understanding of the molecular dynamics of membranes has improved in recent years, both from the experimental as well as the theoretical viewpoints. The development of new experimental contributions have contributed to this, as well as the enormous improvement in the description of membranes using simulation methods. In the experimental field spectroscopic methods (NMR, QENS, IR, fluorescence) and micromechanical (micropipettes) and optical techniques (e.g. videomicroscopy) have provided new insights. In the field of high-frequency dynamics in the THz regime quasielastic neutron scattering (QENS) has been able to demonstrate the existence of a dynamical surface roughness [23] and the existence of collective membrane motions [24] and in this timescale dominant motional contributions were described [25]. NMR relaxation measurements have allowed small rotational motions of membrane components to be elucidated [26, 27, 28, 29].

Although structural aspects of cholesterol in membranes have been investigated in detail (reviewed in [1]), our knowledge of sterol dynamics is quite restricted. Up to the starting point of this project, sterol dynamics had been examined for cholesterol, for which, interestingly, strong anisotropy [30] together with discrete rotation around its long axis [26] were found. It was suggested that these motions are important for the increase of membrane stiffness upon cholesterol insertion [30]. Comparable data for the molecular dynamics of closely structurally-related steroids, such as lanosterol and ergosterol, practically did not exist. However, in one NMR study it was observed that these sterols induce a completely different behaviour of the molecular order parameters of the lipids than does cholesterol [31]. From this one may surmise that ergosterol and lanosterol may exhibit markedly different motional anisotropies in the membrane. Biological membranes suffer from extreme complexity, with many different types of motions existing on similar timescales. In complex molecular systems the molecular dynamics technique has proved to be of considerable use for unravelling details of structure and dynamics. MD simulations had been performed on cholesterol in DPPC and DMPC membranes [20, 22], but not in biologically-relevant sterol concentrations. Moreover, the existing simulations con-

centrated mostly on the effect of the sterol on the bilayer structure, leaving the dynamics of the membrane and of the sterol itself unexamined.

### 3 Aufgabenstellung

The functional form of the force field used in an MD simulation, generally includes a set of empirical parameters which are system dependent and must be tuned prior to performing simulations on a new system or molecule. This tuning step is generally referred to as parametrization of the force field. The reliability of a molecular mechanics calculation is dependent on both the functional form of the force field and on the numerical values of the parameters implemented in the force field itself. Thus, the first necessary step for a reliable MD simulation is the parametrization procedure. Most “all-atom” empirical force fields used in common MD packages (such as CHARMM [32]), are equipped with parameter sets for modelling and combining the basic building blocks of biomolecules, but often not for exotic molecules such as steroids. In the literature only one force field study for cholesterol has appeared for the CFF93 force field which is not widely used [33]. Most of the recently-reported cholesterol:membrane simulations have been using united atom models [19, 20, 34], which might not be suitable for accurate modelling of cholesterol-lipid interactions at an atomic level for comparing with experimental techniques that probe hydrogen-atom dynamics, such as NMR or incoherent neutron scattering. Therefore, the development of a force field for cholesterol, ergosterol and lanosterol was necessary in order to model the lipid-sterol system in a realistic way.

Using MD and QENS the dynamics of structurally-similar biologically relevant sterols and their structural effect in phospholipid membranes are discussed. Central questions concerned the possible different effects of cholesterol, ergosterol and lanosterol on the membrane dynamics and on the structure and order of the membrane. The central technical goal of the proposal was the combination of QENS and MD results on identical sterol/lipid mixtures in a largely-overlapping timescale regime of 4 ns to 100 ps so as to develop a universally applicable model of steroid dynamics in membranes. This required further development of both techniques towards higher sensitivity and resolution (QENS) and state-of-the-art simulations of large systems with accurate potentials and simulation methodology (MD). The criterion for comparison of the techniques will be the dynamical structure factor.

It was possible to monitor the sterol dynamics for cholesterol, ergosterol and lanosterol using QENS with three instrumental resolutions, namely  $1\mu\text{eV}$ ,  $8\mu\text{eV}$  and  $14\mu\text{eV}$ . These resolutions respectively correspond to timescales of 4ns, 800ps and 300ps. The experiment was carried out in 40%mol. sterol concentration and 20%wt hydration at 309K by our collaboration group of Thomas Bayerl in Würzburg [35]. Interestingly, a strong anisotropy in the cholesterol motion was observed together with discrete rotation around its long axis. It was suggested that these motions are important for the increase of the membrane stiffness upon cholesterol insertion. The QENS data for the three sterols also suggest that slight modifications of the sterol structure have a drastic effect on the molecular dynamics of these molecules in lipid bilayers, which in turn may be related to the membrane micromechanical properties. Cholesterol showed an amplitude of its out-of-plane motion

of 1.0-1.1nm, more than a factor of three higher than measured for the other two sterols.

QENS yields information on the same time-scale (1ps - 10ns) as the MD simulation, which makes the comparison straightforward. However, while QENS gives us information on the average dynamic behavior of the molecules, using MD simulations it is possible to decompose the simulation-derived dynamic structure factor into motional components and thus shed light on which particular parts of cholesterol provide the optimal physical properties of the membrane.

Using MD simulations structural and dynamical aspects of cholesterol and ergosterol in DPPC (1,2-dipalmitoylphosphatidylcholine) membranes (Figure 1,2 have been investigated. The 4 systems which were constructed were as follows:

- 200 DPPC membrane with 20% wt hydration (1600 TIP3P [36] water molecules
- 120 DPPC with 80 cholesterol and 1600 TIP3P water molecules
- 120 DPPC with 80 ergosterol and 1600 TIP3P water molecules
- 120 DPPC with 80 lanosterol and 1600 TIP3P water molecules

The results of the simulations have been directly compared with various experimental results.

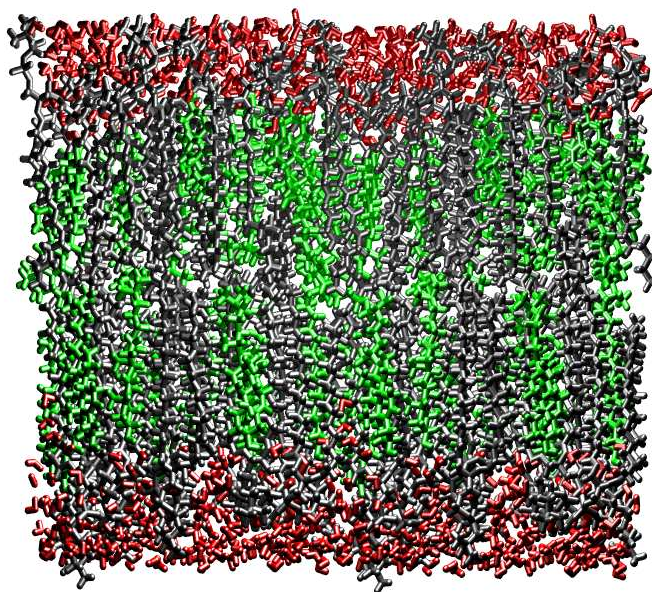


Figure 1: The simulation system. Lipids are shown in grey, cholesterol in green and water in red.

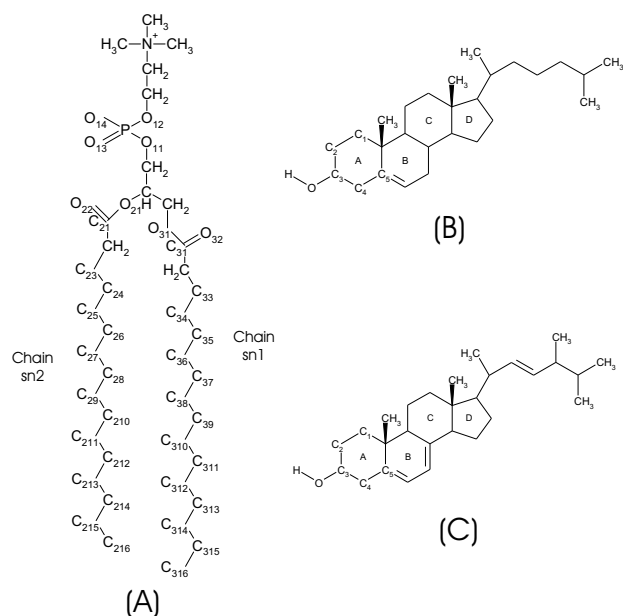


Figure 2: The structures of (A) DPPC, (B) cholesterol and (C) ergosterol

## 4 Planung und Ablauf des Vorhabens

The work-plan for the three-year project was completed as follows:

### First Year

Derivation of force field parameters for cholesterol via automated frequency matching of quantum mechanical and molecular mechanics normal modes. Testing of the force field on experimental X-ray structure. Setting up of the cholesterol/DPPC simulation system. Preliminary heating and equilibration.

### Second Year

Derivation of force field parameters for ergosterol and lanosterol via automated frequency matching of quantum mechanical and molecular mechanics normal modes. Setting up of the ergosterol/DPPC. Setting up a control DPPC simulation with 20%wt. hydration. Preliminary heating and equilibration. Production simulations of cholesterol/DPPC.

### Third Year

Setting up the lanosterol/DPPC simulation system. Setting up a control DPPC simulations with 50%wt. hydration. Preliminary heating and equilibration. Production simulations of ergosterol/DPPC. Analysis of the cholesterol/DPPC simulation and comparison with X-ray, NMR, dilatometry and quasielastic neutron scattering results. Analysis of the ergosterol/DPPC.

## 5 Erzielte Ergebnisse

### 5.1 Force Field development for cholesterol, ergosterol and lanosterol

#### 5.1.1 Computational Details

All quantum chemical calculations were performed with the NWChem 4.5 package [37]. Geometry optimizations and normal mode analysis were performed at the DFT/B3LYP level of theory for the isolated molecules. All molecules except cholesterol have a C1 symmetry. To reduce computational time, the effective core potential (ECP) SBKJG: Stevens-Basch-Krauss-Jasien-Cundari [38] was used for the carbons and the oxygen. ECPs replace the core electrons with an effective potential, thus eliminating the need for calculating the core basis functions, which usually require a large set of Gaussians to describe them. Geometry optimizations were performed to the default tolerances and the frequencies were calculated numerically. A frequency scaling factor of 0.9614 was used to compensate for the use of the harmonic approximation to the potential energy surface [39]. For the calculation of partial atomic charges, all the structures were first optimized at the DFT/6-31G(d) level of theory and then the CHELPG method [40] within NWChem was used to derive them. The Hartree-Fock (HF) method was not preferred for the calculation of the charges as it has been shown that the HF 6-31G\* RESP charges systematically overestimate dipole moments [41]. This is preferred when the system studied is solvated in a polar solvent as the overestimated charges implicitly include the effect of polarization on the molecular charge distribution. However, in an apolar environment like the lipid bilayer the overestimation of the partial charges is not favoured.

The CHELPG method employs a least-squares fitting procedure to determine the set of atomic partial charges that best reproduces the quantum mechanical electrostatic potential at selected grid points. The probe radius of the grid, which determines the envelope around the molecule, was set to 2.5 Å and the grid spacing was 0.1 Å. The grid points for which the QM electrostatic potential is evaluated and used in the fitting procedure of the partial atomic charges all lie outside the van der Waals radius of the atoms and within a cutoff distance from the atomic centers. All grid points that lie within a distance less than 2.5 Å from the surface of the atom were discarded. The fitting was subject to the constraint that the sum of the charges should be equal to the net charge on the molecule. To ensure that the charges on symmetrically equivalent atoms are equal, additional constraints on the partial atomic charges were imposed during the fitting procedure. In particular, the molecule was grouped into subsets of atoms, which were constrained to have zero total charge. For instance, the methyl groups were restrained to zero charge with, in addition, all the hydrogens carrying identical charges.

All molecular mechanics calculations were performed using the CHARMM 27 package [32]. Except for the new parameters which are derived here, the existing CHARMM parameters were used [42, 43, 44, 45]. The molecular mechanics minimizations were carried out using the Steepest Descent algorithm for initial minimization and followed by Newton-Raphson minimization with a convergence criterion for the energy gradient of  $10^{-6}$  kcal/mol/Å. Non-bonded interactions were cutoff at 10 Å with a shifted potential

acting between 10 and 12 Å. Electrostatic interactions were cutoff at 12 Å. In CHARMM the empirical potential energy function is given by Eq.1:

$$\begin{aligned}
V(\mathbf{r}^N) = & \sum_{bonds} K_b(b - b_0)^2 + \sum_{ub} K_{ub}(s - s_0)^2 + \sum_{angles} K_\theta(\theta - \theta_0)^2 + \\
& \sum_{dihedrals} K_\chi(1 + \cos(n\chi - \chi_0)) + \sum_{impropers} K\psi(\psi - \psi_0)^2 + \\
& \sum_{nonbond} \epsilon_{ij} \left[ \left( \frac{R_{ij}^{min}}{r_{ij}} \right)^{12} - \left( \frac{R_{ij}^{min}}{r_{ij}} \right)^6 \right] + \frac{q_i q_j}{D r_{ij}}
\end{aligned} \tag{1}$$

where  $K_b$ ,  $K_{ub}$ ,  $K_\theta$ ,  $K_\chi$ ,  $K_\phi$  are, respectively, the bond, Urey-Bradley, angle, dihedral and improper dihedral constants, and  $b$ ,  $s$ ,  $\theta$ ,  $\chi$ , and  $\phi$  represent, respectively, bond length, Urey-Bradley 1-3 distance, bond angle, dihedral angle and improper torsion angle (the subscript zero were present is used to represent the corresponding equilibrium value). Nonbonded interactions between pairs of atoms (labeled  $i$  and  $j$ ) at a relative distance  $r_{ij}$  are described by the Lennard-Jones 6-12 (LJ) and Coulomb interaction terms.  $R_{ij}^{min}$  and  $\epsilon_{ij}$  are, respectively, the distance between atoms  $i$  and  $j$  at which the LJ potential is minimum and the depth of the LJ potential well for the same pair of atoms.  $D$  is the effective dielectric constant ( $D=1$  in our case) and  $q_i$  the partial atomic charge on atom  $i$ .

### 5.1.2 Automated Frequency Matching Method

The determination of the actual values of the various force constants in Eq.1 is a demanding job. One major difficulty in the development of molecular force fields is that these parameters cannot be directly determined from experiments. The experimental data that pertain to force field calculations, such as infrared frequencies or crystal lattice constants are not a simple function of the force field parameters and they are also rather scarce.

Nonetheless, the force field parameters of the empirical potential energy function, are more directly connected to quantities that are well defined quantum mechanically such as the second derivatives of the energy with respect to coordinates (i.e. the Hessian matrix elements). The point charges of the system can be also readily computed. These quantities are therefore available through *ab initio* calculations, which in this context are invaluable.

Before refinement, an initial set of parameters was determined. The van der Waals constants  $\epsilon_{ij}$  and  $R_{ij}$  depend mostly on atomic properties and are relatively insensitive to changes in the molecular environment. These were directly transferred from original CHARMM values and were not modified during refinement. The second term in Eq.1 (the so-called Urey-Bradley term [42, 43, 44, 45]) is not present in most other force fields and within the CHARMM model its use is limited to a few special cases. Here  $K_{ub}$  was set to zero wherever possible. Equilibrium values for bonds  $b_0$ , angles  $\theta_0$  and dihedrals  $\chi_0$  that were not existing in the original CHARMM force field parameter file [42, 43, 44, 45] were derived from the calculated quantum chemical structure. An initial guess, based on analogy to similar existing CHARMM parameters and on chemical intuition, was made for

all other missing parameters. Equilibrium values and hybridization of the atoms involved should be carefully taken into account when designing a set of initial parameters.

The initial parameter set is used for minimization and calculation of normal modes (eigenvalues and eigenvectors) with CHARMM. The normal modes obtained are then directly compared with the normal modes calculated with the quantum chemistry methods, used as reference values, employing AFMM [46]. Using an iterative procedure, the parameters were thus refined to reproduce the reference set normal modes. One of the major problems of parametrization methods that fit to vibrational frequencies is identifying a calculated mode with the corresponding reference mode. It is possible to obtain good matching of the frequencies for a molecule while exchanging the corresponding eigenvectors. The resulting model would then reproduce well the vibrational frequencies (and the energy) of the reference molecule. However, it may not reproduce the distribution of energy among the inter-molecular modes, and thus the dynamical properties of the molecule. It is therefore important to use a merit function that takes into account both the frequencies and all the corresponding eigenvectors to avoid this problem. AFMM minimizes the above frequency exchange effect. In the “ideal” case of a perfect molecular mechanics model, the vibrational properties of the molecule, as calculated by molecular mechanics, should perfectly match those resulting from the quantum ab initio calculation. For this to occur not only must the frequencies coincide but also the two sets of eigenvectors (resulting from the two different calculations) should coincide. Each eigenvector from the set calculated by molecular mechanics would therefore be orthonormal to all but one (its corresponding eigenvector) of the vectors from the reference set (calculated using quantum chemical methods).

A major requirement in MM force fields is the portability of the parameter set, that is, the possibility to transfer large groups of parameters from one molecule to another. In this respect, addition of new atom types to the force field when designing the new parameter set should be limited only to specific cases in which existing types cannot be used. For the parametrization of the sterols, it was not necessary to define new atom types for CHARMM and the parametrization was based on the already existing lipid atom types. For the  $sp^2$  lipid atoms, the atom type CEL1 was used. For the  $sp^3$  atoms we used the atom types CTL1, CTL2 and CTL3 with one/none (HAL1), two (HAL2), or three (HAL3) hydrogens respectively.

## 5.2 Parametrization Results

### 5.2.1 Parametrization of cholesterol

Parameters for cholesterol were developed using a three step procedure. Initially the AFMM method was used to obtain a first set of parameters. In the second step parameters for the hydroxyl group region were further refined using single point QM energy calculations performed on hexanol. We chose hexanol to model the H-O-C-C rotational energy barrier based on the resemblance of the first cholesterol steroid ring and this molecule. Finally, all remaining parameters were refined using AFMM.

The DFT/B3LYP/SBJKC geometry minimized structure of cholesterol is shown in Fig. 3. The resulting  $v_j^{max}$  vs.  $v_i$  plot for cholesterol is shown in Fig.4. The corresponding

value of  $\sigma=40\text{cm}^{-1}$  is even lower than the range calculated in previous benchmark studies [46].

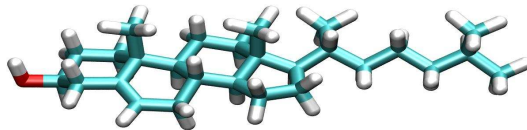


Figure 3: The DFT B3LYP SBJKC geometry optimized structure of cholesterol

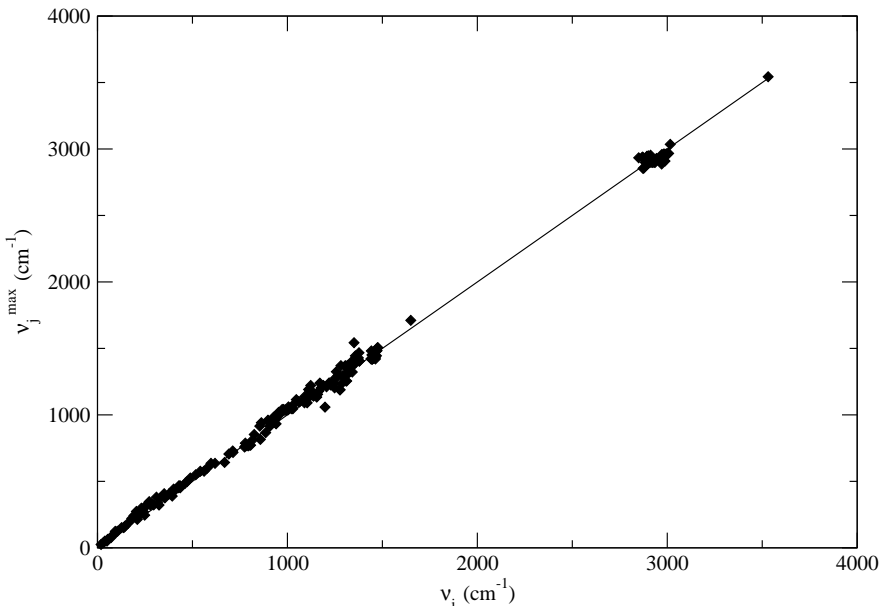


Figure 4:  $v_j^{max}$  vs.  $v_i$  plot for cholesterol. The line is the ideal case of perfectly matched frequencies and eigenvector projections. Points refer to the optimized parameter set.  $\sigma = 40.0\text{cm}^{-1}$

Special care was taken to reproduce correctly the torsional potential of the hydroxyl group region. The rotation around this dihedral is very important because it can determine the residence time and stability of the hydrogen bonds of cholesterol with water and the lipid head group. To check the accuracy of the parameter set in this region, we calculated the rotational energy barrier of the HO - O - C3 - C2 dihedral, using both molecular mechanics and quantum chemistry. To reduce computational time, this calculation was performed using hexanol to model the first sterol ring, and starting parameters previously developed for cholesterol.

The torsional force constants [ $K_\chi$  in Eq. 1] were derived from the energy barrier for rotation of the above-mentioned dihedral at the DFT/SBJKC level of theory using single point calculations to scan the potential energy landscape. The remaining parameters were optimized again in CHARMM using AFMM. An additional term has been added to the dihedral part of the potential to obtain a better fit for the barrier.

## The Cholesterol Crystal Simulation

Final testing of a parameter set should be performed against independent experimental or theoretical data. In this study the refined parameter set was tested by performing an energy minimization and MD simulation of cholesterol in its crystalline state and comparing the results with the X-ray experimental structure [47]. The experimental unit cell with 8 cholesterol molecules (A-H) is triclinic with no symmetry ( $P_1$  symmetry) can be seen in Fig. 5.

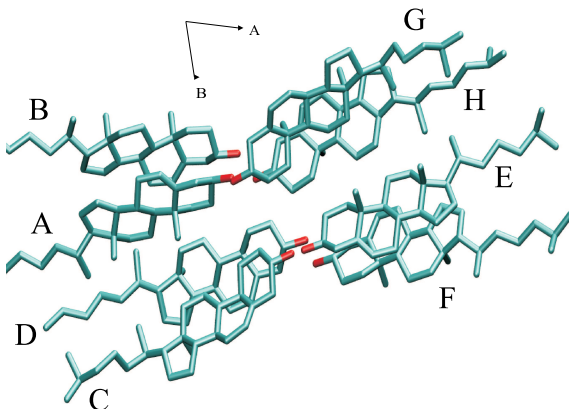


Figure 5: The experimental unit cell of the crystal structure of cholesterol

### Crystal Minimization and Molecular Dynamics

During the calculation the full crystal environment was included using periodic boundary conditions. The unit cell dimensions were allowed to vary during the energy minimization and the molecular dynamics simulation. Hydrogens were constructed using idealized geometric parameters from the hbuild module in CHARMM.

The hydrogen positions, which were not determined experimentally, were constructed within CHARMM. After minimization the cell volume was computed to be  $5056.8 \text{ \AA}^3$ , while the experimental volume is  $5032.8 \text{ \AA}^3$ .

To further test the accuracy of the final parameter set, an MD simulation was performed on the experimental crystal structure. A constant pressure-temperature simulation with periodic boundary conditions was used with a timestep of 0.001 ps to observe the evolution of the crystal cell dimensions. Starting from experimental coordinates, and after minimization the system was heated up to 500 K with 10 K temperature steps. Subsequently, the system was equilibrated for 10 ps using velocity rescaling followed by a second phase of equilibration without velocity rescaling for 10 more ps at 298 K (experimental temperature). Finally, production dynamics followed for 2ns at 298 K. The calculated cell vectors are reproduced within 2.4% of experimental values and with a maximum standard deviation of  $\pm 0.5 \text{ \AA}$  and  $1.85^\circ$  for the MD. We were also able to reproduce characteristic

features of the crystal structure such as the rigidity of the sterol ring and the hydrogen bonded network of the crystal.

### 5.2.2 Parametrization of ergosterol

The DFT/B3LYP/SBJKC geometry minimized structure of ergosterol is shown in Fig. 6. For the parametrization of ergosterol the already optimized cholesterol parameters were used. For the parameters which were still missing, the ergosterol molecule was truncated only to the part of the missing parameters to save computational time. Therefore, the molecule that was parametrized was 2,3,3a,4,5,5a,6,9b-octahydro-3a,6-dimethyl-1H-cyclopenta[a]naphthalene. The resulting  $v_j^{max}$  vs.  $v_i$  plot for this molecule is shown in Fig.4. The corresponding value of  $\sigma=84.1cm^{-1}$  is within the range of the previous benchmark studies [46]. Points that deviate from the ideal plot may indicate exchanged or mismatched frequencies. A crystal simulation on the ergosterol crystal structure was not possible because of the poor experimental data quality which gave several bonds greater than 1.7 Å.

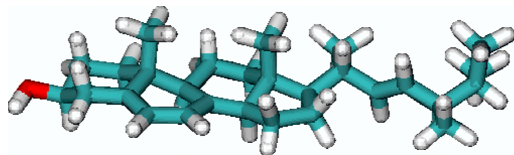


Figure 6: The DFT B3LYP SBJKC geometry optimized structure of ergosterol

### 5.2.3 Parametrization of Lanosterol

#### Frequency Matching and Rotational Energy Barrier

For the parametrization of lanosterol, the previous parameters developed for both cholesterol and ergosterol were applied were needed. For reasons of computational efficiency lanosterol was split into two smaller molecules: 2,2 dimethyl cyclohexanol and 3 isopropyl-2-methyl-hex-2-ene. The resulting  $v_j^{max}$  vs.  $v_i$  plots for the two molecules are shown in Figs. 8 and 9.

As in the case of cholesterol, we have calculated the rotational energy barrier of the HO - O - C3 - C2 dihedral, using both molecular mechanics and quantum chemistry. To reduce computational time, this calculation was performed using 2,2 dimethyl cyclohexanol to model the first sterol ring.

The torsional force constants [ $K_\chi$  in Eq. 1] were derived from the energy barrier for rotation of the above-mentioned dihedral at the DFT/SBJKC level of theory using single point calculations to scan the potential energy landscape. In the case of lanosterol two additional dihedral terms were included to the potential to obtain a better fit for the barrier. The parameters used to reproduce this rotational barrier were then fixed and the remaining ones were optimized again in CHARMM using AFMM.

### 800K MD in vacuo of cholesterol, ergosterol and lanosterol

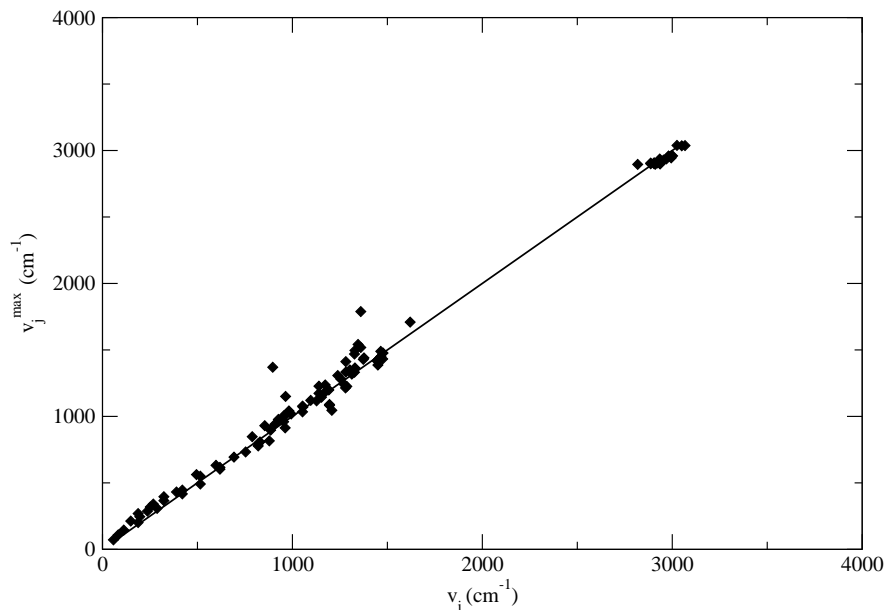


Figure 7:  $v_j^{max}$  vs.  $v_i$  plot for 2,3,3a,4,5,5a,6,9b-octahydro-3a,6-dimethyl-1H-cyclopenta[a]naphthalene. The line is the ideal case of perfectly matched frequencies and eigenvector projections. Points refer to the optimized parameter set.  $\sigma = 84.1cm^{-1}$

It has been shown that the chiral conformation of biologically important sterols is essential for its *in vivo* function [48]. Therefore it is important that the sterols preserve their stereochemistry during an MD simulation. In previous MD studies of cholesterol in bilayers [49] simulation artifacts resulting in an inversion of the asymmetrical centers in were observed. Therefore, to ensure that the chirality of the molecule is maintained and to test the new parameter set we performed a 2ns MD simulation series of the single cholesterol, ergosterol and lanosterol molecule, respectively, *in vacuo* at 800K. The steroid ring systems were found to be rigid and not to undergo major conformational changes. The flexible hydrocarbon tails were found to undergo several conformational changes as expected. During the simulation, the stereochemistry of all the seven asymmetrical centers was preserved in all three sterols eben at these extreme conditions.

## 5.3 Molecular Dynamics of Cholesterol and Ergosterol in DPPC membranes

### 5.3.1 Computational Details

To construct the cholesterol-DPPC system we used coordinates of DPPC molecules determined by Sundaralingam [50]. Coordinates for the cholesterol molecule were taken from the crystal structure by Shieh et al. [47]. The initial configuration was created by duplicating, flipping and translating two original molecules with no specific ordering. In this arrangement we are not biased towards any particular configuration of the system, as up to now there is no sufficient evidence on the ordering of cholesterol in the membrane.

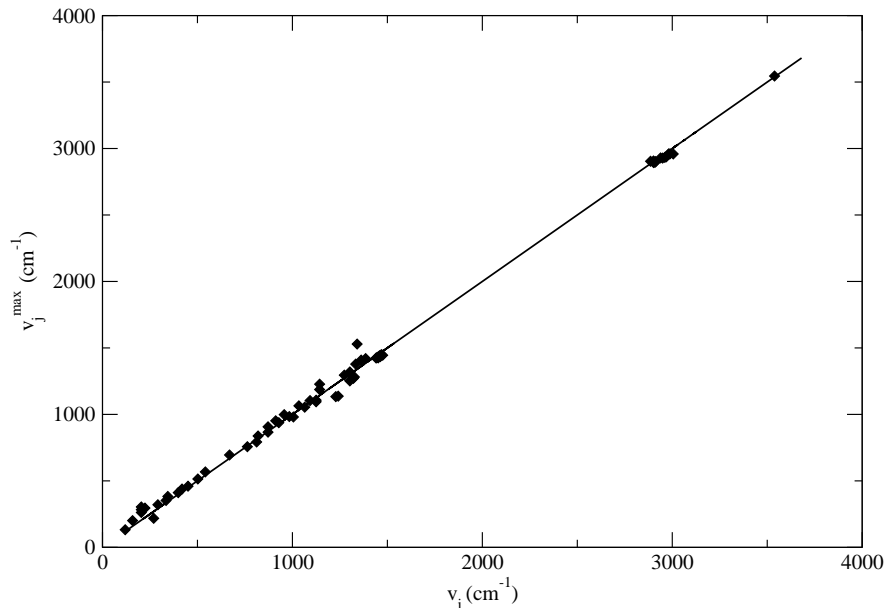


Figure 8:  $v_j^{max}$  vs.  $v_i$  plot for 2,2 dimethyl hexanol. The line is the ideal case of perfectly matched frequencies and eigenvector projections. Points refer to the optimized parameter set.  $\sigma = 41.2\text{cm}^{-1}$

Cholesterol was initially placed so that its hydroxyl group is in the same depth with the glycerol backbone of DPPC. A concentration of 40%mol cholesterol and 20% wt hydration were chosen to match the experimental setup. We used the CHARMM 22 force field for DPPC and our derived force field for cholesterol [51]. Partial atomic charges were calculated using NWchem 4.1 at the 6-31G(d) basis set level and the CHELPG analysis. The water model employed in the simulations was TIP3P [36].

Using this setup an initial system of 50 lipids and 400 water molecules was created, which was then successively minimized and heated and was finally equilibrated for 600 ps at constant pressure (1 atm) and temperature (Nose Hoover thermostat at 309 K) with periodic boundary conditions. We kept angles of the simulation cell fixed and varied the dimensions of the cell using a Hoover barostat. The particle-mesh ewald summation technique was employed to calculate electrostatic contributions. The van der Waals interactions were cut off at 13 Å with the shift smoothing function. The non-bonded pair list was set up to 14 Å. After the 600 ps equilibration, a 200-lipid system was created by duplicating and translating the original slab of the pre-equilibrated 50 lipids. After equilibration we performed a production run for 25 ns using the above-mentioned simulation details.

The ergosterol-DPPC system was created by replacing all cholesterol molecules of an equilibrated configuration with ergosterol. A concentration of 40%mol cholesterol and ergosterol, respectively and 20% wt hydration were chosen to match the experimental setup. We used the CHARMM 22 force field for DPPC and our derived force fields for cholesterol and ergosterol [51]. Partial atomic charges were calculated using NChem 4.5 at the 6-31G(d) basis set level and the CHELPG analysis. The water model employed

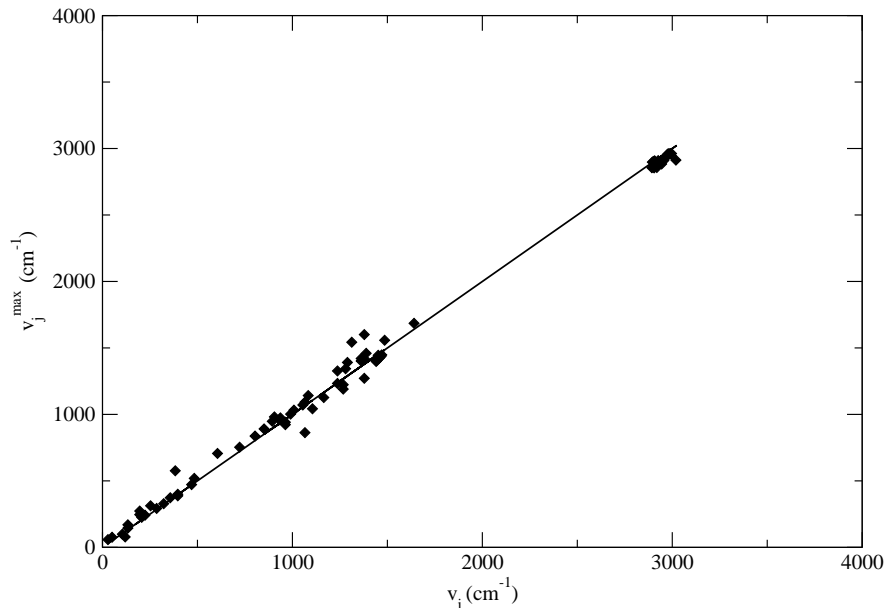


Figure 9:  $v_j^{max}$  vs.  $v_i$  plot for 1,2 isopropyl-1-pentene. The line is the ideal case of perfectly matched frequencies and eigenvector projections. Points refer to the optimized parameter set.  $\sigma = 61.2cm^{-1}$

in the simulations was TIP3P [36]. The ergosterol-DPPC system was successively minimized and heated and was finally equilibrated for 2ns at constant pressure (1atm) and temperature (Nose Hoover thermostat at 309K) with periodic boundary conditions. After that a production run for 1ns was completed. We kept angles of the simulation cell fixed and varied the dimensions of the cell using a Hoover barostat. The particle-mesh ewald summation technique was employed to calculate electrostatic contributions. The van der Waals interactions were cut off at  $13\text{\AA}$  with the shift smoothing function. The non-bonded pair list was set up to  $14\text{\AA}$ .

After equilibration we performed a production run for 10 ns using the above-mentioned simulation details.

Calculations were performed on HELICS, IWR - Universitt Heidelberg (HBFG funds, hww cooperation) using the CHARMM simulation package version 28b1 [32].

### 5.3.2 Volume and Surface Area per Lipid

There is no obvious solution of how to calculate the “Surface Area per Lipid” in a mixture of two components such as the DPPC-cholesterol system or for an ergosterol-DPPC system. A simple approach to the problem is given as follows: The area occupied by a DPPC molecule in the bilayer can be written in terms of volume and thickness as:

$$A_{DPPC}(x) = \frac{2V_{DPPC}(x)}{h(x)} \quad (2)$$

where  $V_{DPPC}$  is the volume of the lipid and  $h(x)$  is the average thickness of the membrane which corresponds to the average distance of two phosphorus atoms in opposite layers.

The volume that a DPPC molecule occupies in the membrane could be calculated as follows:

$$V_L = \frac{V_T - N_W \cdot V_W - N_C \cdot V_C}{N_L} \quad (3)$$

where  $V_T$  is the total volume of the system in each frame of the trajectory,  $N_L = 120$  the total number of the lipids,  $N_W = 1600$  the number of waters,  $V_W = 29.9 \text{ \AA}^3$  the volume of one water molecule and  $N_C = 80$  the number of cholesterol/ergosterol molecules. The volume of a cholesterol molecule,  $V_C = 629.1 \text{ \AA}^3$  and the volume of an ergosterol molecule,  $V_C = 659.2$  is given from the crystallographic data [52, 53]. In this approach we consider  $V_W$  and  $V_C$  fixed as cholesterol and ergosterol are fairly rigid bodies.

For the cholesterol-DPPC system, the mean volume of DPPC was found to be  $1176.4 \pm 5.2 \text{ \AA}^3$  (all deviations refer to standard deviations) and the mean surface area per lipid is  $47.0 \pm 0.2 \text{ \AA}^2$ . For the ergosterol-DPPC system, the mean volume was found to be  $1154.4 \pm 5.3$  and mean surface area per lipid  $46.1 \pm 0.2 \text{ \AA}^2$ . For both systems, the bilayer thickness was found to be  $50.0 \text{ \AA}$  by calculating the distance of the two peaks of the electron density profile.

### 5.3.3 Deuterium Order Parameters

The most popular quantity to characterize the order of the hydrocarbon chains in lipid bilayers is the deuterium NMR order parameters. Such an order parameter may be defined for every  $\text{CH}_2$  group in the chains as:

$$S_{CD}^i = \frac{1}{2}(3\langle \cos^2 \theta_{CD}^i \rangle - 1) \quad (4)$$

where  $\theta_{CD}^i$  is the angle between a CD-bond (in the experiment) or a CH-bond (in the simulation) of the  $i$ th carbon on the acyl chain and the membrane normal (z-axis). The brackets indicate averaging over the two bonds in each  $\text{CH}_2$  group, all the lipids and time.

This property was calculated from the MD trajectory of the cholesterol/DPPC, ergosterol/DPPC systems and pure DPPC systems. The order parameter profile shows that cholesterol and ergosterol apply an ordering effect on the lipid hydrocarbon chain. For the pure DPPC system the ordering of the chain with respect to the z-axis is significantly lower. Our results show good overall agreement with those obtained in the studies of Urbina et al. [31] and Faure et al. [54]. Our order parameter profile is also consistent with all simulation results obtained for similar conditions [20, 19, 34, 21].

### 5.3.4 Electron Density Profiles

The first atomic scale picture of the average structure of the lipid bilayer:water interface can be produced as a measurement of the density distributions of different types of atoms along the bilayer normal (z-axis) by neutron and X-ray diffraction studies. The corresponding electron density profile for the bilayer has been provided by our MD simulation and is in good agreement with experimental results obtained by various experimental groups.

The electron density profile is calculated every 1 ps and averaged out in the trajectory by dividing the simulation cells into  $0.5 \text{ \AA}$  slabs and determining the time-averaged number

of electrons in each slab. The peaks show the electron-rich phosphate region of the headgroup. Defining the bilayer thickness as the distance between the peaks in the total electron density, we obtain 50.0 Å which is slightly bigger than the values determined by X-ray diffraction analysis and by Smondyrev et al. [20] and Hofsäss et al. [55].

### 5.3.5 Cholesterol and Ergosterol Tilt Angle

We also measured the distribution of the tilt of cholesterol in the lipid bilayer. The tilt is defined as the angle between the bilayer normal and the vector connecting carbon atoms  $C_3$  and  $C_{17}$  in the sterol ring system. The average cholesterol tilt angle in the DPPC membrane is 10.0° and for ergosterol 8.1°. The tilt angle value for cholesterol is very close to the one measured by Smondyrev and Berkowitz [19], 10.6°, for a DMPC bilayer. However it is much lower than the value measured by the same group for 11% cholesterol in DMPC (22.2°). The study of Murari et al. [8] for 1:1 DPPC:Chol mixture at 24°C obtains an average cholesterol tilt of 16° from quadrupolar splittings.

### 5.3.6 Radial Distribution Functions

The water in the polar lipid region solvates the polar lipid head groups. These interactions can be best described by radial distribution functions for the water oxygen surrounding the phosphate P, choline N, carbonyl C, and cholesterol hydroxyl H atoms. The radial distribution function (rdf) between atom  $x$  and atom  $y$  is defined as the average over all  $x$  atoms in the system of the distance from an  $x$  atom to each other  $y$  atom. The distances between the atoms on different molecules were binned and the resulting rdf was normalized by dividing by  $4\pi r^2 dr$  in which  $r$  is the distance in the middle of the bin and  $dr$  in the bin width, set at 0.07 Å. The volume around each particle is divided into concentric spherical shells, and the number of particles in each shell is counted and divided by the shell volume (given by the difference between two spherical volumes), to obtain the local density. The densities at each distance are then averaged over all particles, and normalised with the overall density to obtain  $g(r)$ . Thus,  $g(r)$  is given by the equation:

$$g(r) = \frac{1}{\rho^2 \frac{4}{3}((r + r^3 dr)^3 - (r - r^3 dr)^3)} \frac{1}{N} \sum_{i=1}^N N_j$$

where  $N_j$  is the number of particles and  $j$  such that  $|r + dr| > |r_i - r_j| > |r - dr|$

The cholesterol hydroxyl H and the water O  $g(r)$  has a sharp first peak at 2 Å, indicating tight solvation shell around the hydroxyl of cholesterol of 3 water molecules (obtained by integrating  $g(r)$  to the first minimum). By integrating the corresponding  $g(r)$  functions to the first minimum we also obtain 1.3 waters around the phosphate O, 1.4 waters around the choline N and 0.6 waters around carbon C21 of the sn2 chain of DPPC.

## 5.4 Dynamical Analysis of the System

### 5.4.1 QENS of Cholesterol-DPPC Bilayers - Oriented Bilayer Dynamics

To measure the anisotropy of the sterol motion and take full advantage of the use of oriented multilayer samples, the QENS experiment took place in two specific orientations

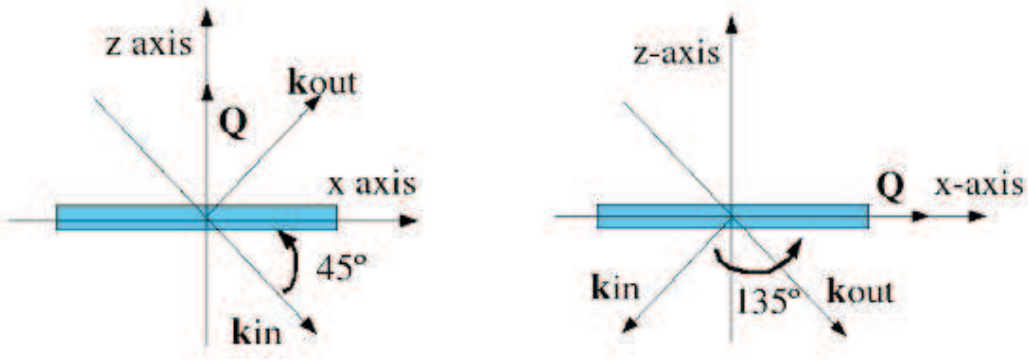


Figure 10: The elastic momentum transfer vector  $\vec{Q}$  is in (a) parallel and in (b) perpendicular to the membrane plane, if scattered neutrons (wave vector  $\vec{k}_1$  are detected at  $\phi = 90^\circ$  with respect to the incident wave vector  $\vec{k}_0$

of the sample with respect to the incident neutron beam. The scattering geometry is schematically depicted in in Figure 10. At an orientation of  $135^\circ$  between the incident and neutron beam and the membrane normal, the momentum transfer is mainly directed perpendicular to the membrane normal [i.e. parallel to the bilayer plane (x-y plane)]. In this case, the in-plane (lateral) motion of the sterol under study will dominate the incoherent scattering. On the other hand, at an orientation of  $45^\circ$  the momentum transfer is mainly parallel to the membrane normal, and thus the incoherent scattering is dominated by out-of plane motion of the sterol along the z-direction (membrane normal).

The calculations should therefore be done for a specific orientation of  $\vec{Q}$ . The intermediate scattering function needs to be calculated only for the  $Q_x, Q_y, Q_z$  components of this  $Q$  and not to be averaged as in the case of isotropic media.

For the  $45^\circ$  orientation, if we consider the incident beam to have coordinates  $\vec{k}_{in} = (k\cos 45^\circ, 0, -k\cos 45^\circ)$  and the scattered wave vector  $\vec{k}_{out} = (k\cos 45^\circ, 0, k\cos 45^\circ)$ , then  $\vec{Q} = (Q_x, Q_y, Q_z)$  becomes according to the relation  $\vec{Q} = \vec{k}_{out} - \vec{k}_{in}$ :

$$\vec{Q} = k(0, 0, \sqrt{2}) = \frac{2\pi}{\lambda}\sqrt{2}(0, 0, 1) \quad (5)$$

For the  $135^\circ$  orientation, if we consider the incident beam to have coordinates  $\vec{k}_{in} = (-k\cos 45^\circ, 0, k\cos 45^\circ)$  and the scattered wave vector  $\vec{k}_{out} = (k\cos 45^\circ, 0, k\cos 45^\circ)$ , then  $\vec{Q} = (Q_x, Q_y, Q_z)$  becomes according to the relation  $\vec{Q} = \vec{k}_{out} - \vec{k}_{in}$ :

$$\vec{Q} = k(\sqrt{2}, 0, 0) = \frac{2\pi}{\lambda}\sqrt{2}(1, 0, 0) \quad (6)$$

In order to compare with experimental data, the intermediate scattering function was calculated with nMoldyn ??:

$$I_{inc}(\vec{Q}, t) = \langle e^{i\vec{Q}\cdot\vec{r}(t)} e^{-i\vec{Q}\cdot\vec{r}(0)} \rangle \quad (7)$$

The Fourier transform of  $I_{inc}(\vec{Q}, t)$  gives the dynamic structure factor:

$$S(\vec{Q}, \omega) = \frac{1}{2\pi} \int_{-\infty}^{\infty} dt e^{-i\omega t} I_{inc}(\vec{Q}, t) \quad (8)$$

IN5, Resolution = 14meV,  $\lambda = 10\text{\AA}^{-1}$ ,  $\theta = 45^\circ$

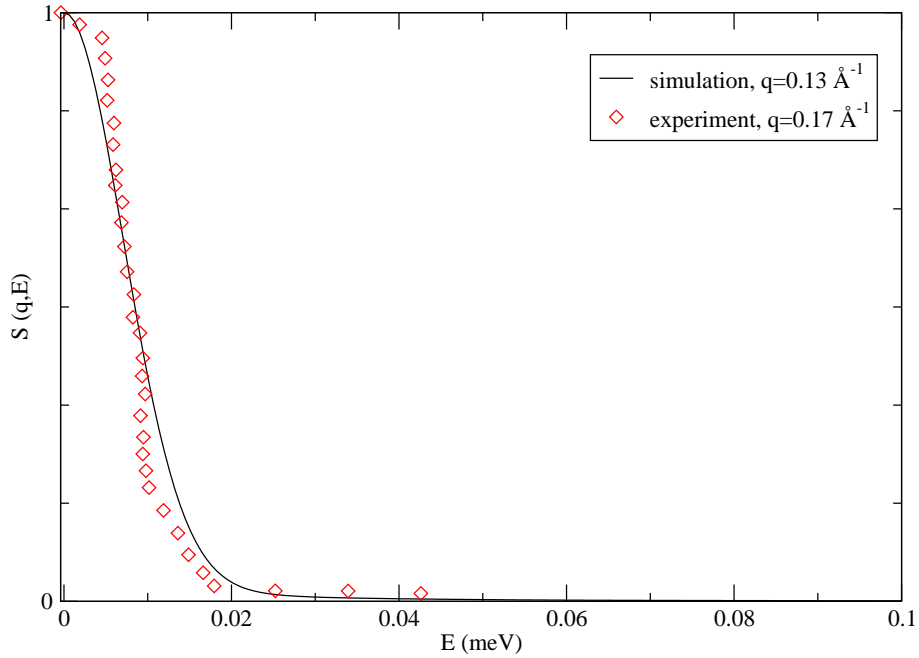


Figure 11: Comparison of experimental and simulation structure factor

In Figure 11 the experimental spectra and the calculated spectra from the cholesterol-DPPC trajectory are depicted.

The elastic incoherent structure factor (EISF) is defined as the limit of the incoherent intermediate scattering function for infinite time:

$$EISF(\vec{Q}) \doteq \lim_{t \rightarrow \infty} I_{inc} \quad (9)$$

The total elastic intensity (within instrumental resolution) as a function of the scattering vector contains information on the geometry of the motions integrated over the time corresponding to the instrumental resolution. For computational purposes it is convenient to use the following definition:

$$EISF(\vec{Q}) = \frac{1}{N} \sum_{\alpha} \langle |e^{i\vec{Q} \cdot \vec{r}_{\alpha}}|^2 \rangle \quad (10)$$

where infinitely good resolution ( $\Delta E=0$ ) is assumed.

The EISF is experimentally accessible as the ratio of the elastically scattered intensity to the sum of elastically and quasielastically scattered intensity. This definition neglects inelastic scattering:

$$A_0(\vec{Q}) \doteq \frac{\mathcal{S}_{inc}^{el}(\vec{Q})}{\mathcal{S}_{inc}^{el}(\vec{Q}) + \mathcal{S}_{inc}^{qe}(\vec{Q})} \quad (11)$$

## EISF, IN5, $\theta = 45^\circ$

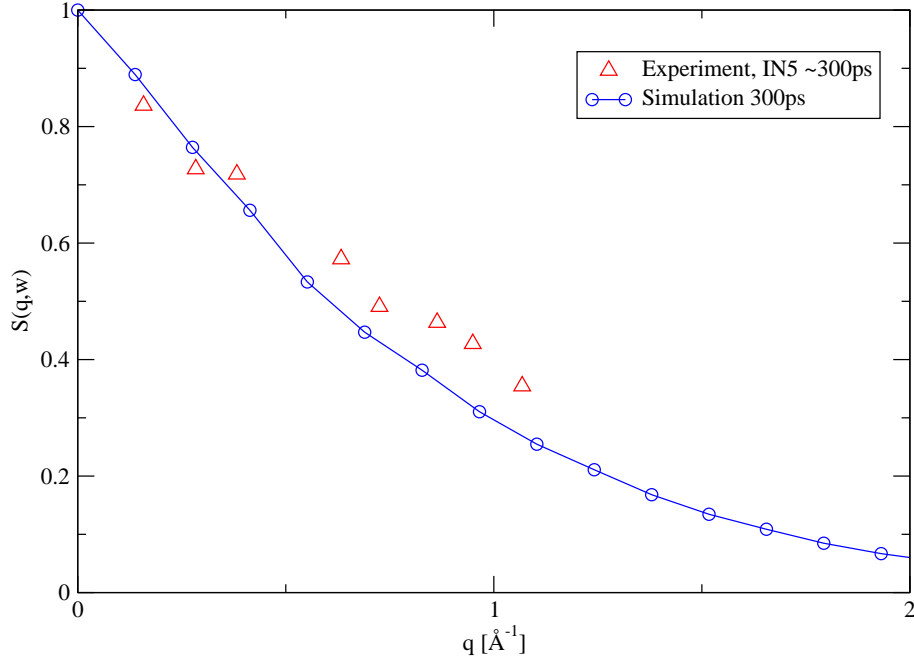


Figure 12: EISF for total system

where  $\mathcal{S}_{inc}^{el}(\vec{Q})$  and  $\mathcal{S}_{inc}^{qe}(\vec{Q})$  are the integrated intensities corresponding to the elastic and quasielastic part of the spectra, respectively.

The EISF was then calculated from the theoretical approach and compared with the experimental result [35] (Fig.12). For the theoretical approach a trajectory of 300ps was used.

### 5.4.2 Mean Square Displacement

The Mean Square Displacement (MSD) is a measure of the average distance a molecule or an atom travels in time. It is defined as:

$$MSD(t) = \langle \Delta \vec{r}_i(t)^2 \rangle = \langle (\vec{r}_i(t) - \vec{r}_i(0))^2 \rangle \quad (12)$$

In the case of linear increase of the MSD with time the MSD can be quantified in terms of the diffusion constant from the slope of the curve:

$$\lim_{t \rightarrow \infty} \frac{d}{dt} \langle \Delta \vec{r}_i(t)^2 \rangle \quad (13)$$

The MSD autocorrelation functions for the DPPC Carbons were calculated for three simulation systems namely cholesterol/DPPC, ergosterol/DPPC and pure DPPC for trajectories of 4ns. Interestingly, we observed that upon insertion of cholesterol or ergosterol in the membrane system the MSD of the DPPC carbons increased. In other words, although from the order parameter profiles cholesterol and ergosterol seem to induce more order in the membrane, it seems that they provide DPPC with more flexibility.

## 5.5 Ausblick

A new force field for cholesterol, ergosterol and lanosterol has been derived using an automated frequency matching method that compares quantum mechanical normal modes with molecular mechanical normal modes. The cholesterol parameters were successfully tested on the cholesterol crystal. A publication with all the final parameter sets is in preparation ("A new force field for biologically-important sterols" by Z.Cournia, J.C. Smith and G.M. Ullmann). A preliminary parameter set for cholesterol has already been published ("Derivation of a new force field for cholesterol", by Z.Cournia, A.C. Vaiana, G.M. Ullmann and J.C. Smith, *Pure Appl.Chem.* 1, 2004) In this framework a new program for molecular mechanics force field parametrization was written and can be used for parametrization of new molecules. A description of this program has been accepted for publication in the *Computer Physics Communications* journal. Molecular mechanics parameterization is a tedious but necessary task in the case of missing parameters. The new parameter sets have enabled us to perform realistic sterol:membrane MD simulations.

Molecular Dynamics simulations have helped us to gain better insight on the effect of cholesterol and ergosterol in the membranes. As a starting point we have calculated properties of the simulated system which could be directly compared to experimental results. The surface area per lipid was compared with dilatometry experiments, electron density profiles from x-ray scattering, order parameter profiles from NMR, and the structure factor from QENS. In all cases we were within very good agreement with the experimental results. One of the major results was that we have been able to observe the "ordering" effect that cholesterol and ergosterol induce on the hydrocarbon lipid chains. While the pure DPPC system is significantly disordered by means of the hydrocarbon chains being aligned to the membrane normal, upon insertion of cholesterol the chains become stiffer giving more rigidity to the system. Ergosterol exhibited slightly more ordering on the lipid chains, possibly as a result of its more rigid steroid ring (has one extra double bond than cholesterol). It is clear that by this effect the two sterols can regulate the membrane's fluidity. Ergosterol's tilt angle was also found to be more aligned with the membrane normal than the one for cholesterol.

QENS has been performed on the cholesterol/d75-DPPC, ergosterol/d75-DPPC and lanosterol/d75-DPPC systems with application of different energy resolutions i.e. timescales. The average molecular dynamics of the three sterols was therefore studied in these timescales. The structure factor for the cholesterol/d75-DPPC system for the 300ps timescale was calculated from MD simulations and compared with the experiment. Since the agreement was good, the calculation of the structure factor for the other two resolutions and also for the ergosterol/DPPC system will be done. Since QENS gives us information on the average dynamic behavior of the molecules, a further analysis of the structure factor would include decomposition of the simulation-derived structure factor into motional components (rotational, translational, internal) and thus shed light on which particular parts of cholesterol provide the optimal physical properties of the membrane. Future prospects include modeling and understanding more complex systems (e.g. cholesterol, lipid and membrane proteins). The mean square displacement results for the control DPPC system and for the cholesterol/DPPC system showed that although cholesterol makes the membrane stiffer by inducing order on the lipid hydrocarbon chains, at the same time

it provides the membrane with the required flexibility so as to allow binding and lateral mobility of membrane proteins. A publication containing the above-mentioned results on structural and dynamical effects of sterols in the membrane is planned within the next few months.

Das diesem Bericht zugrundeliegende Vorhaben wurde mit Mitteln des Bundesministeriums fuer Bildung und Forschung unter dem Foerderkennzeichen 03SHE2HD gefoerdert. Die Verantwortung fuer den Inhalt dieser Veroeffentlichung liegt beim Autor.

## References

- [1] L. Finegold. *Cholesterol in Membrane Models*. CRC Press, Boca Barton, FL, 1985.
- [2] D.W. Russell and K. D. Setschell. Bile acid biosynthesis. *Biochemistry*, 31:4737–4749, 1992.
- [3] K. Schoonjans, C. Brendel, D. Mangelsdorf, and J. Anxwerx. Sterols and gene expression: Control of affluence. *Biochim. Biophys. Acta*, 1529:114–125, 2000.
- [4] A. Kusumi, M. Tsuda, T. Akino, O. Ohnishi, and Y. Terayama. Protein-phospholipid-cholesterol interaction in the photolysis of invertebrate rhodopsin. *Biochemistry*, 22:1165–1170, 1983.
- [5] K. Simons and D. Toomre. Lipid rafts and signal transduction. *Nature Rev. Mol. Cell Biol.*, 1:31–39, 2000.
- [6] T.H. Haines. Do sterols reduce proton and sodium leaks through lipid bilayers? *Prog. Lipid Res.*, 40:299–324, 2001.
- [7] K. Bloch. *Cholesterol, evolution of structure and function.*, pages 1–24. in *Biochemistry of Lipids and Membranes*, Eds. J. E. Vance and D. E. Vance, Benjamin/Cummins Pub. Co. Inc., New York, 1985.
- [8] R. Murari, M. Murari, and W.J. Baumann. Sterol orientations in phosphatidylcholine liposomes as determined by deuterium NMR. *Biochemistry*, 25:1062, 1986.
- [9] J.M. Polson, I. Vattulainen, H. Zhu, and H. Zuckermann. Simulation study of lateral diffusion in lipid-sterol bilayer mixtures. *Eur. Phys. J. E.*, 5:485–497, 2001.
- [10] M.R. Vist and J.H. Davis. Phase equilibria od cholesterol/dipalmitoylphosphatidylcholine mixtures:  $^2\text{H}$  nuclear magnetic resonance and differential scanning calorimetry. *Biochemistry*, 29:451–464, 1990.
- [11] M.J. Zuckermann, J.H. Ipsen, and O.G. Mouritsen. *Theoretical studies of the phase behavior of lipid bilayers containing cholesterol*, pages 223–256. CRC Press, Boca Barton, FL, 1993.

- [12] L. Miao, M. Nielsen, J. Thewalt, J.H. Ipsen, M. Bloom, M.J. Zuckermann, and O.G. Mouritsen. From lanosterol to cholesterol: structural evolution and differential effects on lipid bilayers. *Biophys. J.*, 82:1429–1444, 2002.
- [13] J.F. Nagle and S. Tristram-Nagle. Structure of lipid bilayers. *Biochim. Biophys. Acta*, 1469:159–195, 2000.
- [14] S. Tristram-Nagle and J.F. Nagle. Lipid bilayers: thermodynamics, structure, fluctuations and interactions. *Chemistry and Physics of Lipids*, 127:3–14, 2004.
- [15] J. Baudry, E. Tajkhorshid, F. Molnar, J. Phillips, and K. Schulten. Molecular Dynamics Study of Bacteriorhodopsin and the Purple Membrane. *J. Phys. Chem. B*, 105:908, 2001.
- [16] D. Mihailescu and J.C. Smith. Atomic detail peptide-membrane interactions: Molecular Dynamics of gramicidine S in a DMPC bilayer. *Biophys. J.*, 79:1718, 2000.
- [17] S. Berneche, M. Nina, and B. Roux. Molecular Dynamics simulation of melittin in a dimyristoyl phosphatidylcholine bilayer membrane. *Biophys. J.*, 75:1603, 1998.
- [18] L. Forrest, A. Kukol, I. Arkin, A. Tielman, and M. Sansom. Exploring the models of Influenza M2 channel - MD Simulations in a phospholipid bilayer. *Biophys. J.*, 78:79, 2000.
- [19] A. Smondyrev and M. L. Berkowitz. MD Simulation of the structure of DMPC bilayers with Cholesterol, Ergosterol, and Lanosterol. *Biophys. J.*, 80:1649, 2001.
- [20] A.M. Smondyrev and M.L. Berkowitz. Structure of DPPC/Cholesterol bilayer at low and high cholesterol concentrations: molecular dynamics simulation. *Biophys. J.*, 77:2075, 1999.
- [21] S. W. Chiu, E. Jacobsson, and H. L. Scott. Combined MC and MD simulation of hydrated lipid-cholesterol lipid bilayers at low Cholesterol concentration. *Biophys. J.*, 80:1104, 2001.
- [22] K. Tu, M. Klein, and D. Tobias. Constant-Pressure MD investigation of Cholesterol effects in a DPPC bilayer. *Biophys. J.*, 75:2147, 1998.
- [23] S. Koenig, W. Pfeiffer, T.M. Bayerl, D. Richter, and E. Sackmann. Molecular dynamics of lipid bilayers studied by incoherent quasi-elastic neutron scattering. *Journal de Physique II France*, 2:1589–1615, 1992.
- [24] W. Pfeiffer, S. Knig, J. F. Legrand, T. M. Bayerl, D. Richter, and E. Sackmann. Neutron spin echo study of membrane undulations in lipid multibilayers. *Europhys. Lett.*, 23:457–462, 1993.
- [25] S. Knig, T.M. Bayerl, G. Coddens, D. Richter, and E. Sackmann. Hydration dependence of chain dynamics and local diffusion in L- $\alpha$  DPPC multibilayers studied by incoherent quasi-elastic neutron scattering. *Biophys. J.*, 68:1871–1880, 1995.

- [26] M. Brown. Anisotropic nuclear spin relaxation of cholesterol in phospholipid bilayers. *Molec. Phys.*, 71:903–908, 1990.
- [27] M. Bloom and J. Thewalt. Spectroscopic determination of lipid dynamics in membranes. *Chemistry and Physics of Lipids*, 73:27–38, 1994.
- [28] E.J. Dufourc, C. Mayer, J. Stohrer, G. Althoff, and G. Kothe. Dynamics of Phosphate Head Groups in Biomembranes - Comprehensive Analysis Using Phosphorus-31 Nuclear Magnetic Resonance Lineshape and Relaxation Time Measurements. *Bio-phys. J.*, 61:42–57, 1992.
- [29] M.F. Brown. *Membrane structure and dynamics studied with NMR spectroscopy*, pages 175–252. Birkhaeuser, Basel, 1996.
- [30] C. Gliss, O. Raneidl, H. Casalta, E. Sackmann, R. Zorn, and T. Bayerl. Anisotropic motion of cholesterol in oriented DPPC bilayers studies by quasielastic neutron scattering: the liquid-ordered phase. *Biophys. J.*, 77:331, 1999.
- [31] J.A. Urbina, S. Pekerar, H. Le, J. Patterson, B. Montez, and E. Oldfield. Molecular order and dynamics of phosphatidylcholine bilayer membranes in the presence of cholesterol, ergosterol and lanosterol: a comparative study using  $^2\text{H}$ -,  $^{13}\text{C}$ - and  $^{31}\text{P}$ -NMR spectroscopy. *Biochim. Biophys. Acta*, 1238:163, 1995.
- [32] B. R. Brooks, R. Bruccoleri, B. D. Olafson, D. J. States, S. Swaminathan, and M. Karplus. CHARMM: A Program for Macromolecular Energy, Minimization and Dynamics Calculations. *J. Comp. Biol.*, 4:187, 1983.
- [33] C. Liang, L. Yan, J.R. Hill, C. S. Ewig, T.R. Stouch, and A. T. Hagler. Force Field studies of cholesterol and cholesteryl acetate crystals and cholesterol-cholesterol intermolecular interactions. *J. Comp. Chem.*, 16:883–897, 1995.
- [34] M. Pasenkiewicz-Gierula, T. Rog, K. Kitamura, and A. Kusumi. Cholesterol Effects on the PC Bilayer polar region: A MD study. *Biophys. J.*, 78:1376, 2000.
- [35] E. Endress, H. Heller, H. Casalta, M. F. Brown, and T. M. Bayerl. Anisotropic motion and molecular dynamics of cholesterol, lanosterol and ergosterol in lecithin bilayers studied by quasi-elastic neutron scattering. *Biochemistry*, 41:13078, 2002.
- [36] W.L. Jorgensen, J. Chandrasekhar, J.D. Madura, R.W. Impey, and M.L. Klein. Comparison of simple potential functions for simulating liquid water. *J. Chem. Phys.*, 79:926, 1983.
- [37] R. J. Harrison, J. A. Nichols, T. P. Straatsma, M. Dupuis, E. J. Bylaska, G. I. Fann, T. L. Windus, E. Apra, J. Anchell, D. Bernholdt, P. Borowski, T. Clark, D. Clerc, H. Dachsel, B. de Jong, M. Deegan, K. Dyall, D. Elwood, H. Fruchtl, E. Glendenning, M. Gutowski, A. Hess, J. Jaffe, B. Johnson, J. Ju, R. Kendall, R. Kobayashi, R. Kutteh, Z. Lin, R. Littlefield, X. Long, B. Meng, J. Nieplocha, S. Niu, M. Rosing, G. Sandrone, M. Stave, H. Taylor, G. Thomas, J. van Lenthe, K. Wolinski, A. Wong,

- and Z. Zhang. NWChem, A Computational Chemistry Package for Parallel Computers, Version 4.0.1. *Pacific Northwest National Laboratory, Richland, Washington, USA*, 2001.
- [38] W.J Stevens, H. Basch, and M. Krauss. . *J. Chem. Phys.*, 81:6026, 1984.
- [39] <http://srdata.nist.gov/cccbdb>. *National Institute of Standards and Technology, USA*, 2004.
- [40] C.N. Breneman and K.B. Wiberg. . *J. Comp. Chem.*, 11:361, 1990.
- [41] P. Cieplak, J. Caldwell, and P. Kollman. Molecular Mechanics Models for organic and biological systems going beyond the atom centered two body additive approximation: Aqueous solution free energies of methanol and N-methyl acetamide, nucleic acid base and amide hydrogen bonding and chloroform/water partition coefficients of the nucleic acid bases. *J. Comp. Chem.*, 22:1048–1057, 2001.
- [42] S.E. Feller, G. Gawrisch, and Jr. A.D. MacKerell. Polyunsaturated Fatty Acids in Lipid Bilayers: Intrinsic and Environmental Contributions to their Unique Physical Properties. *J. Am. Chem. Soc.*, 124(2):318, 2002.
- [43] S.E. Feller and Jr. A.D. MacKerell. An Improved Empirical Potential Energy Function for Molecular Simulations of Phospholipids. *J. Phys. Chem. B*, 104:7510, 2000.
- [44] D. Yin and Jr. A.D. MacKerell. Combined Ab Initio/Empirical Approach for Optimization of Lennard-Jones Parameters. *J. Comp. Chem.*, 19:334, 1997.
- [45] S.E. Feller, D. Yin, R.W. Pastor, and Jr. A.D. MacKerell. Molecular Dynamics Simulation of Unsaturated Lipid Bilayers at Low Hydration: Parametrization and Comparison with Diffraction Studies. *Biophys. J.*, 73:2269, 1997.
- [46] A.C. Vaiana, A. Schulz, J. Worfrum, M.Sauer, and J.C. Smith. Molecular mechanics force field parametrization of the fluorescent probe rhodamine 6G using automated frequency matching. *J. Comp. Chem.*, 24:632, 2002.
- [47] H. Shieh, L.G. Hoard, and C.E. Nordman. The structure of cholesterol. *Acta Cryst.*, B37:1538, 1981.
- [48] C.M. Crowder, E.J. Westover, A.S. Kumar, Jr. R.E Ostlund, and D.F Covey. Enantiospecificity of cholesterol function in vivo. *J. Biol. Chem.*, 276:44369, 2001.
- [49] T. Rog and M. Pasenkiewicz-Gierula. Cholesterol effects on the phosphatidylcholine bilayer nonpolar region: a molecular simulation study. *Biophys. J.*, 81:2190, 2001.
- [50] M. Sundaralingam. Molecular structures and conformations of the phospholipids and shingomyelins. *Ann. N. Y. Acad. Sci.*, 195:324, 1972.
- [51] Zoe Cournia, Andrea Vaiana, Jeremy C. Smith, and G. Matthias Ullmann. Derivation of a molecular mechanics force field for cholesterol. *Pure Appl. Chem.*, 76(1):189, 2004.

- [52] H.S. Shieh, L.G. Hoard, and C.E. Nordman. Crystal structure of anhydrous cholesterol. *Nature*, 267:287–289, 1977.
- [53] S.E. Hull and M.M. Woolfson. The crystal structure of ergosterol monohydrate. *Acta Cryst.*, B32:2370–2373, 1976.
- [54] C. Faure, J. Transchant, and E.J. Dufourc. Comparative effects of cholesterol and cholesterol sulfate on hydration and ordering of DMPC membranes. *Biophys. J.*, 70:1380, 1996.
- [55] C.Hofsaess, E. Lindahl, and O. Edholm. Molecular dynamics simulations of phospholipid bilayers with cholesterol. *Biophys. J.*, 84:2192, 2003.